MATERIALE PLASTICE
https://revmaterialeplastice.ro
https://doi.org/10.37358/Mat.Plast.1964

Design of Melamine Foam/Perforated Plates Composite Absorber for Effective Sound Absorption Performance

XUELIANG JIANG[1,2], QIANG FU[1,2], DAN WU[1,2], GUIJIANG TANG[1,2], FENG YOU[1,2], CHU YAO[1,2]*

[1]Hubei Key Laboratory of Plasma Chemistry and Advanced Materials, Wuhan Institute of Technology, 206 Guanggu 1 Road, East Lake New Technology Development Zone, 430205, Wuhan, China
[2]College of Materials Science and Engineering, Wuhan Institute of Technology, 206 Guanggu 1 Road, East Lake New Technology Development Zone, 430205, Wuhan, China

Abstract: *To give full play to the advantages of perforated plate backed by porous materials in low and medium frequency noise absorption, this study uses Johnson-Champoux-Allard method with the finite element model to describe the acoustic characteristics of this composite structure. The effects of structural parameters of perforated plate and characteristic parameters of melamine foam on sound absorption coefficient were systematically investigated by numerical simulation. Practical composite were prepared to verify the reliability of the numerical simulation method. The simulation and experimental data in this study are helpful to promote the design of porous material-perforated plate structure for noise control in life.*

Keywords: *perforated plates, porous materials, numerical simulation, sound absorption*

1. Introduction

Noise is an important interference factor in life and work. In order to solve noise pollution problem, great efforts have been put into the research of various sound absorption materials and methods. In this regard, porous sound absorbing materials, resonant sound absorbing structures and composite structure have been widely used due to their outstanding advantages in sound absorption [1-3].

Many porous materials have been studied for acoustic absorption such as organic fibers [4-7] (wool, quartz, hemp, etc.), inorganic fibers (glass wool, metal fibers, etc.), polymer foam, metal foam and composite foams. The excellent sound absorption effect of porous acoustic materials is mainly derived from the effective dissipation of acoustic energy, which includes the synergistic effect of various mechanisms. It can be briefly summarized as two parts of of viscoelastic frame damping and visco-inertial and thermal damping [8,9]. For the first part, sound waves cause vibrations in the porous structure, and friction between solid molecules. For the second part, friction between air medium and porous material wall is caused due to the viscosity of air medium [10]. However, the sound absorption ability of porous structures is poor for medium and low frequencies below 2000 Hz, due to low frequencies cause more structural vibration than air friction. Fortunately, the resonant sound absorbers possess a high absorption coefficient of sound waves near the resonant frequency, which has great advantages in absorbing low frequency noise. However, resonant sound absorbers usually have the disadvantage of narrow sound absorption bandwidth. Therefore, composite materials composed of porous materials and the resonant sound absorbers with specially designed structure is desirably needed to realize broadband sound absorption. Nevertheless, adequate thickness and complex structure makes the combined composites difficult to design to achieve excellent sound absorption performance.

The microstructure of porous materials is the main factor to influence acoustic properties of porous materials. Building appropriate models to simulate the microstructure can help to design or predict the acoustic properties of porous materials. Through the analysis of propagation and dissipation process of sound waves in porous materials, the semi-phenomenological model [11-13] (like Johnson-Champoux-Allard (JCA) model) containing basic acoustic parameters is proposed to characterize sound absorption properties of the porous materials. Periodic Unit cells (PUC's) and the Finite Element Method (FEM) have become the effective methods to study the relationship between microstructure and macroscopic

**email: chuyao@wit.edu.cn*

acoustic properties. K.Gao et al. [14] proposed the method of measuring and simulating the micro-structure characterization and homogenization of acoustic polyurethane foam, and established two PUC's model - fully open and partially open Kelvin units with thin film - to represent foam. And they [15] also studied the relationship between the microstructure of foamed plastics and the macroscopic acoustic properties using a PUC's model, revealing that the relationship depends on the microscopic boundary conditions. Ju et al. [9] used crystal clusters formed by the Kelvin unit model to simulate foam structure, they adjusted the opening degree of PUC's by eliminating cell walls randomly, and explored the relationship between polyurethane foam's openness and sound absorption properties. Some simplified PUC's model is also used for research, hoping to reduce the difficulty of modeling when meeting the requirements like in [16–18]. People also study and design some novel composite and periodic structures to realize the controllability of noise absorption [19-21].

PUC's about perforated plates have been proposed for studying the sound absorption properties. Rostand et al. [22] proposed an expression that can properly explain the hole interaction and non-uniform distribution effect by PUC's and FEM. It is found that under low sound field excitation, the interaction effect between holes is closely related to the hole spacing and distribution. Wang et al. [23] used the homogeneous physical velocity porous media (PVPM) model to describe the acoustic characteristics of porous plates. The finite element method can effectively study the distribution and mechanism of acoustic energy dissipation in resonant absorber. The energy loss is mainly distributed at the interface abrupt change, i.e. the empty edge [24, 25]. In order to improve the sound absorption performance, the back cavity of the sound absorber is specially designed. J. Carbajo et al. [26] separated the back cavity with a micro perforated plate to improve the effective sound absorption bandwidth of the perforated plate. Gai et al. [27] introduced the L-shaped structure after the micro perforated plate cavity to divide the cavity, and studied the sound absorption characteristics of the L-shaped split cavity structure MPP. Kim et al. [28] constructed a perforated plate with multiple hole sizes (two and four hole sizes) and composed a back cavity segmented by porous materials. Ming et al. [29] designed a sound absorbers with a micro-perforated panel backed by an array of parallel-arranged sub-cavities at different depths. Li et al. [30] combined porous materials, micro-perforated panel and extended tubes, the sound absorption performance of low and middle frequency is improved.

In this paper, the composite sound-absorbing structure with porous materials filled in the cavity behind the perforated plate is designed. The finite element model of composite structure is established for numerical simulation. The effects of characteristic parameters of porous materials and the structural parameters of perforated plate of the composite structure on the sound absorption performance are systematically explored. Moreover, practical composites absorbers combing melamine foam and perforated plates are prepared to verify the simulated results. The simulation and experimental data in this study can provide reference for the design of composite structure to achieve excellent sound absorption performance for the noise control.

2.Materials and methods

2.1. Acoustic model and methodology

2.1.1. Semi-empirical equivalent fluid model

As a classical five-parameter semi-empirical equivalent fluid model, the Johnson-Champoux-Allard (JCA) model is adopted in this study [27-29]. The effective density $\rho(\omega)$ and effective volume modulus $K(\omega)$ expressed by the model are as follows:

$$\rho(\omega)=\alpha_\infty\rho_o\left[1+\frac{\sigma\phi}{j\omega\rho_o\alpha_\infty}\left(1+\frac{4i\alpha_\infty^{\,2}\eta\omega\rho_o}{(\sigma\phi\Lambda)^2}\right)^{1/2}\right] \quad (1)$$

$$K(\omega)=kp_0\left(k-(k-1)\left[1+\frac{\sigma'\phi}{i\omega\rho_o\alpha_\infty N_{pr}}\left(1+\frac{4i\alpha_\infty^2\eta N_{pr}\omega\rho_o}{(\sigma'\Lambda'\phi)^2}\right)^{1/2}\right]^{-1}\right)^{-1} \quad (2)$$

$$\sigma'=\frac{8\eta\alpha_\infty}{\Lambda'^2\phi} \quad (3)$$

where ϕ is porosity, α_∞ is (inertial) tortuosity, σ is flow resistivity, Λ (VCL, L_V) is viscosity characteristic length, and Λ' (TCL, L_{th}) is thermal characteristic length. ω is the angular frequency, N_{pr} is Prandtl number, k is the heat capacity ratio of air, η is the viscosity of air, p_0 is the ambient pressure, ρ_o is the air density.

Positive incidence characteristic impedance Z_c and wavenumber k_c can be expressed as follows:

$$Z_c=\sqrt{\rho_{(\omega)}\cdot K_{(\omega)}} \quad (4)$$

$$k_c=\omega\sqrt{\frac{\rho_{(\omega)}}{K_{(\omega)}}} \quad (5)$$

where $\rho(\omega)$ and $K(\omega)$ are get from equations (1) and (2).

Considering that porous materials are backed by rigid walls and the acoustic wave is incident vertically, the sound absorption coefficient (α) of materials can be obtained by the surface impedance method:

$$Z_n=-i\frac{Z_{eq}}{\rho_0 c_0}\cot g\left(k_{eq}L_s\right) \quad (6)$$

$$\alpha=1-\left|\frac{Z_n-1}{Z_n+1}\right|^2 \quad (7)$$

where Z_n is normal incidence specific surface impedance, c_0 is air sound velocity, L_s is material thickness, Z_{eq} is characteristic impedance, and k_{eq} is wave number.

2.1.2. Finite element model of composite structured

The finite element model of perforated plate backed by melamine foam is established. Periodicity and symmetry of composite structures are used to reduce the calculation amount. Figure 1 shows a quarter of the finite element model. The model is composed of four. The top part is the perfect matching layer (PML), the second part is the sound field, the third part is perforated plate, and the bottom part is melamine foam. The visco-thermal acoustic-frequency domain module is used in the perforated part, and the pressure acoustic-frequency domain module is used both in the air domain and melamine foam domain.

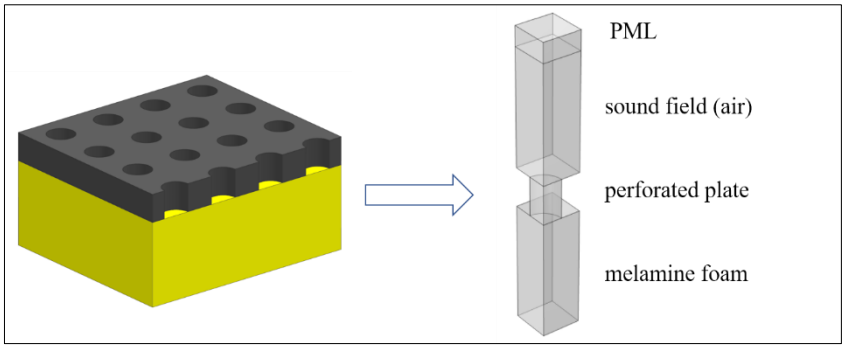

Figure 1. A quarter of the finite element model

2.1.3. Influencing parameters of perforated plate

The control variable method is used to study the influencing parameter of perforated plate. For the melamine foam part, the low-density melamine foam (LDMF) with the thickness of 30 mm is set. The corresponding basic acoustic parameters are listed in Table 1.

The perforation distribution of the perforation plate is shown in Figure 2. The perforation is evenly distributed. The perforation rate (δ) can be calculated from equation (8):

$$\delta = \frac{\pi a^2}{L_x L_y} \tag{8}$$

where a is radius, L_x and L_y are center distance, and $L_x = L_y$.

Table 1. Basic acoustic parameters of low-density melamine foam (LDMF) and high-density melamine foam (HDMF)

	ρ/kg/m^2	ϕ	σ/Pa·s/m^2	α_∞	Λ/um	Λ'/um
LDMF	7.59	0.997	7478	1	139.3	164.8
HDMF	14.7	0.992	24400	1	34.9	107.3

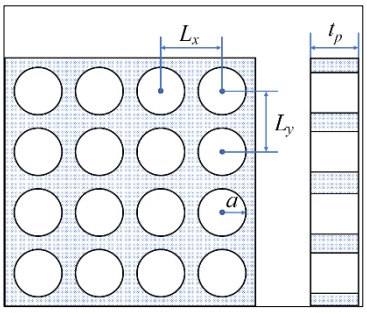

Figure 2. Schematic picture of the perforated plates

2.1.4. Influencing parameter parameters design of melamine foam

Five basic acoustic characteristics of the porous material are used in the JCA model and the control variable method is employed for discussion. Two kinds of perforated plates, the one with advantages in low frequency sound absorption (called L-perforated plates) with parameters δ = 0.05, a = 2 mm, t_p = 10 mm, and the other one with advantages in medium frequency sound absorption (called M-perforated plates) with parameters δ = 0.15, a = 1 mm, t_p = 5 mm are designed in this study.

3. Results and discussions

3.1. Simulation analysis of perforated plate structural parameters on acoustic performance

Simulation analysis in this paper is based on COMSOL Multiphysics. To study the effect of perforation rate δ of perforated plate on the acoustic performance of the composite, six perforation rates

are designed under two kinds of aperture (a = 1 and 2 mm, respectively) with the thickness of perforated plate fixed as 5 mm. The data are listed in Table 2 calculated from equation (8). Figure 3 shows the influence of δ on the sound absorption coefficient of the composite. The curve profiles exhibit similar spectral characteristics with two aperture sizes. The lower the perforation rate is, the sharper the sound absorption coefficient curve becomes. Moreover, at the lower the perforation rate, the peak value gets higher and the resonance peak is closer to the low frequency. The sound absorption coefficient equal to or greater than 0.98 is regarded as complete sound absorption. Notably, when in the cases of δ = 0.05, a = 1, f = 710 Hz and a = 2, f = 630~710 Hz, the maximum sound absorption coefficient is 0.99 and 0.98 respectively, which indicates that the absorbers can achieve complete sound absorption. The average sound absorption coefficient is used to evaluate the sound absorption performance in the corresponding frequency band. The average sound absorption coefficient of low frequency (180~500 Hz) and middle frequency (500~2000 Hz) was represented as α_L and α_M, respectively. As can be seen from Figure 3c and 3d, the α_L value decreases whereas the α_M value increases both at two different aperture sizes with the increase of perforation rate. This suggests that the adsorption performance is related to perforation rate. In addition, with the same perforation rate, the α_L value with a=2 mm is higher than that with a=1 mm, while the α_M value has the inverse trend, demonstrating that the pore size of the perforated plate can affect the absorption performance of the composite.

Table 2. The parameters of δ and $L_x(L_y)$ in the two case of a = 1 and 2 mm calcuyalted from equation (8)

(a)a = 1 mm	δ	0.05	0.10	0.15	0.20	0.25	0.30
	L_x=L_y/mm	7.93	5.60	4.58	3.96	3.54	3.24
(b)a = 2 mm	δ	0.05	0.10	0.15	0.20	0.25	0.30
	L_x=L_y/mm	15.85	11.21	9.15	7.93	7.09	6.47

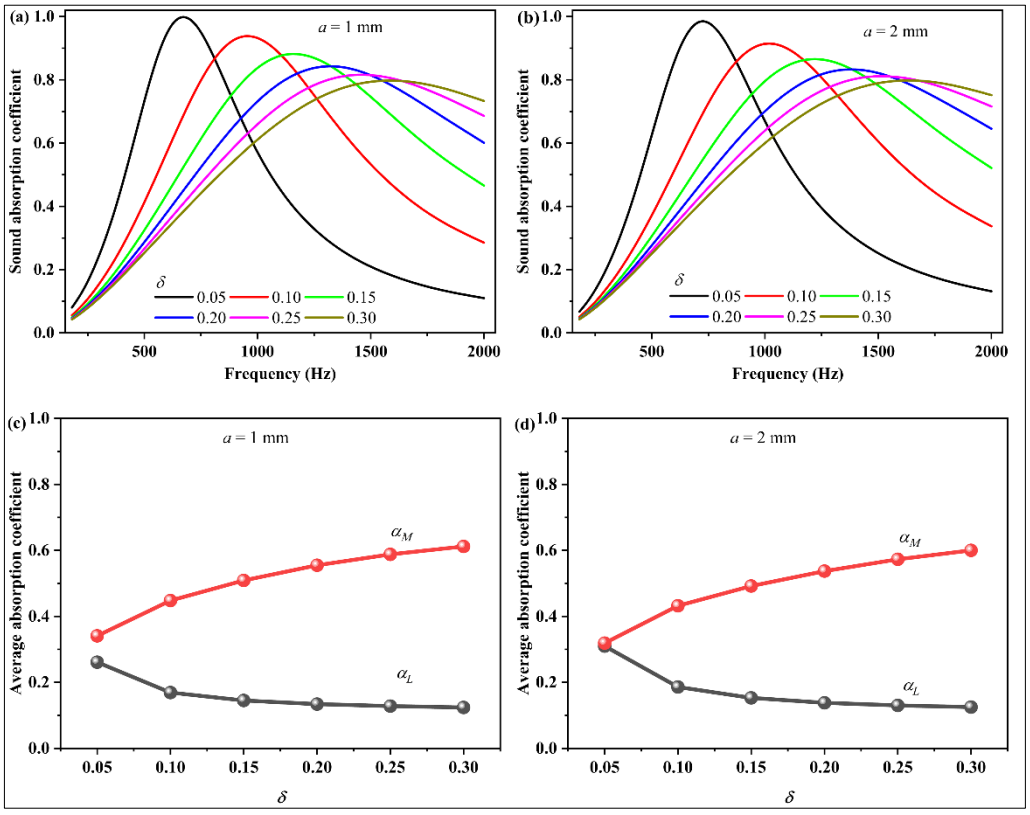

Figure 3. The Influence of perforation rate (δ) with (a) a = 1 mm and (b) a = 2 mm on sound absorption coefficient, and the average absorption coefficient α_L and α_M as a function of δ with pore size of (c) a = 1 mm and (d) a = 2 mm

The influence of pore size on the sound absorption coefficient is further explored. Six pore sizes are designed at two perforation rates with the thickness of perforated plate fixed as 5 mm. The data are listed in Table 3 calculated from equation (8). As shown in Figure 4, the sound absorption curve becomes narrow and sharp and the spectra peak moves towards the low frequency with the increased size of aperture. In Figure 4a, the maximum sound adsorption coefficient for a = 0.5, 1, 2, 3 mm is 0.99, 0.98, 0.99, 0.99, respectively, revealing that complete sound absorption can be reached for the composite. However, with further bigger pore size (a = 4.00 and 5.00 mm), the maximum sound absorption is degenerated (0.97 and 0.95, respectively). In Figure 4b, the maximum acoustic absorption coefficient successively increases from 0.87, 0.88, and 0.90 to 0.95 with the increase of aperture from 1 to 5 mm. However, the maximum acoustic absorption coefficient is 0.89 with a = 0.50 mm. The effect of pore size on the average sound absorption coefficient at low and medium frequencies is also summarized. As can be seen from Figure 4c and 4d, the α_L increases with the increase of pore size at both perforation rates, and the increase is more obvious when the perforation rate is lower. The α_M decreases with the increase of aperture, and the decrease is more obvious when the perforation rate is lower. So we can determine that lower perforation rate and larger aperture are favorable for low frequency sound absorption, while higher perforation rate and smaller aperture are favorable for medium frequency sound absorption.

Table 3. The parameters of a and $L_x(L_y)$ in the two case of δ = 0.05 and 0.15 calculated from equation (8)

(a) δ = 0.05	a/mm	0.50	1.00	2.00	3.00	4.00	5.00
	$L_x = L_y$/mm	3.96	7.93	15.85	23.78	31.71	39.63
(b) δ = 0.15	a/mm	0.50	1.00	2.00	3.00	4.00	5.00
	$L_x = L_y$/mm	2.29	4.58	9.15	13.73	18.31	22.88

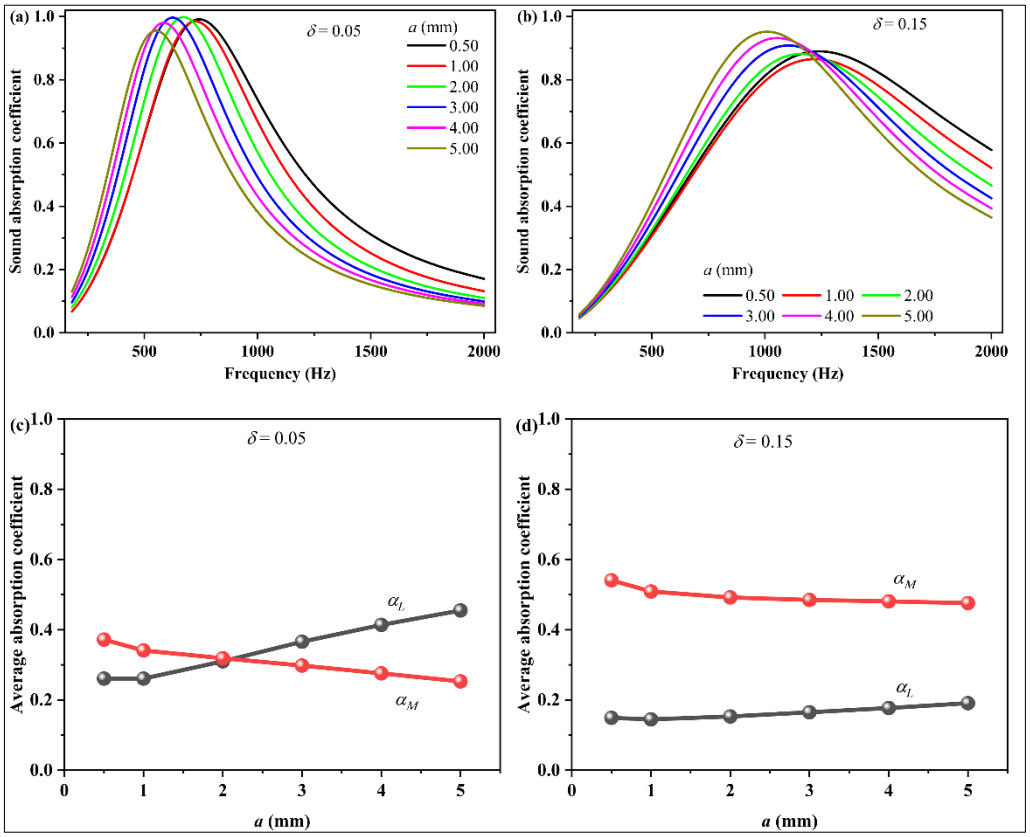

Figure 4. The Influence of aperture size (a) with (a) δ = 0.05 and (b) δ = 0.15 on sound absorption coefficient, and the average absorption coefficient α_L and α_M as a function of a with perforation rate of with (c) δ = 0.05 and (d) δ = 0.15

The thickness of perforated plate is an important factor affecting the sound absorption performance of the composite. Six kinds of perforated plate thicknesses are selected under the combination of different perforation rate and aperture with data listed in Table 4. The simulation results are shown in Figure 5. As the thickness of the perforated plate increases, the curve becomes sharp, the sound absorption bandwidth becomes narrow, and the absorption peak moves to low frequency. Specifically, the sound absorption peak locates at 500 Hz at t_p=8 mm, which is the boundary between low frequency and intermediate frequency (Figure 5a). Moreover, all of the maximum sound absorption coefficients are about 0.95, manifesting excellent sound insult performance of the composites. In Figure 5b, the shape of the curves changes dramatically with the increase of thickness. In the case of δ = 0.15 a = 0.5 mm, Figure 5b displays that the maximum sound absorption coefficient increased from 0.84 to 0.98 with the increase of perforated plate thickness from 2 to 17 mm, and the sound absorption peak moves from 1700 to 720 Hz. This shows that when the perforation rate is high and the aperture is small, the sound absorption is very sensitive to the thickness.

The Figure 5c and 5d display that the α_L increases with the increase of thickness at both combination of perforation rate and aperture, and the α_M decreases with the increase of thickness. We can conclude that the perforated plate with lower perforation rate, larger aperture and larger thickness (called L-perforated plate) has advantages in low frequency sound absorption, while the perforated plate with higher perforation rate, smaller aperture and smaller plate thickness (called L-perforated plate) has advantages in medium frequency sound absorption.

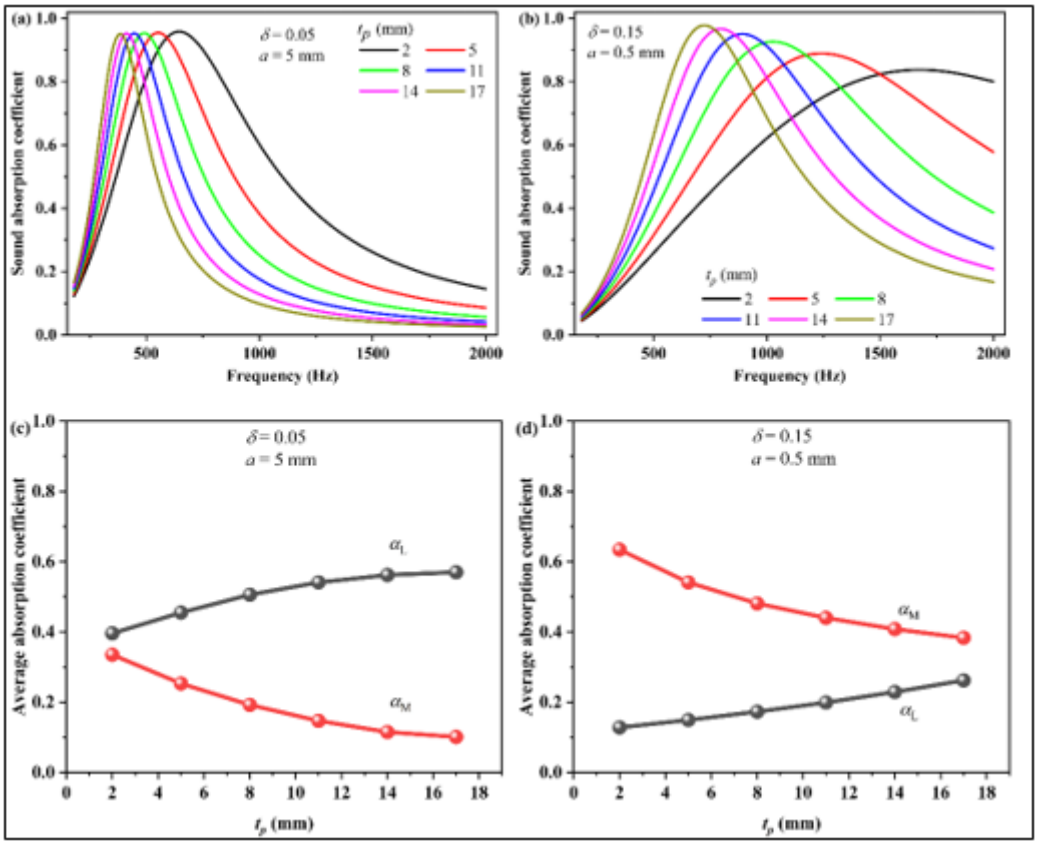

Figure 5. The Influence of thickness (t_p) with (a) δ = 0.05, a = 5 mm and (b) δ = 0.15, a = 0.5 mm on sound absorption coefficient, and the average absorption coefficient α_L and α_M as a function of t_p with perforation rate of with (c) δ = 0.05, a = 5 mm and (d) δ = 0.15, a = 0.5 mm

3.2. Simulation analysis of influencing parameters of melamine foam on acoustic performance

The traditional perforated plate theory suggests that filling the porous material in the back cavity of the perforated plate can adjust the acoustic resistance ratio of the perforated plate [31]. Filling the porous

material means changing the medium in the back cavity of the composite. In other words, the acoustic waves in the back cavity change from propagating in the air to propagating in the porous material, which are equivalent to increasing the sound volume of the body cavity, so that the resonance frequency of the perforated plate decreases. To analyze the influence of porosity (ϕ), tortuosity (α_∞), flow resistivity (σ), viscous characteristic length (Λ), and thermal characteristic length (Λ') of melamine foam on the acoustic performance of the composite, the corresponding experimental scheme is designed and the data are given in Tables 4-8.

Porosity refers to the percentage of air in porous materials. High porosity is an important characteristic of porous materials, and it gives porous materials a very large specific surface area which is conducive to thermal-viscous dissipation. Figure 6 shows the effect of porosity on the sound absorption coefficient. With the increase of porosity, sound absorption peaks move to low frequency under both perforated plate conditions. For the L-perforated plate the maximum sound absorption coefficient almost always reaches 1 (Figure 6a), illustrating the excellent sound insulate properties. However, for the M-perforated plate, the maximum sound absorption coefficient decreases with the increase of porosity (Figure 6b).

The influence of porosity on the average sound absorption coefficient at low and medium frequencies are shown in Figure 6c and 6d. Obviously, for L-perforated plate, α_M increases and α_L decreases with the increase of porosity, while both α_L and α_M increase with increasing porosity for M-perforated plate. So for L-perforated plate, higher porosity has advantages in low frequency sound absorption and lower porosity has advantages in medium frequency sound absorption. For M-perforated plate, higher porosity has slight advantages in both low and medium frequency sound absorption.

Table 4. The parameters of t_p in the two case of δ = 0.05 a = 5 mm and δ = 0.15 a = 0.5 mm

	t_p/mm					
(a) δ = 0.05 a = 5 mm	2	5	8	11	14	17
(b) δ = 0.15 a = 0.5 mm	2	5	8	11	14	17

Table 5. Perforated plate parameters and porosity design

	porosity/ ϕ					
(a)δ =0.05 a = 2 mm t_p = 10 mm	0.75	0.8	0.85	0.9	0.95	0.99
(b)δ =0.15 a =1 mm t_p =5 mm	0.75	0.8	0.85	0.9	0.95	0.99

Table 6. Perforated plate parameters and tortuosity design

	tortuosity/α_∞					
(a)δ =0.05 a = 2 mm t_p = 10 mm	1	1.05	1.1	1.15	1.2	1.25
(b)δ =0.15 a =1 mm t_p =5 mm	1	1.05	1.1	1.15	1.2	1.25

Table 7. Perforated plate parameters and flow resistivity design

	flow resistance/σ/Pa·s/m²					
(a)δ =0.05 a = 2 mm t_p = 10 mm	5000	10000	15000	20000	25000	30000
(b)δ =0.15 a =1 mm t_p =5 mm	5000	10000	15000	20000	25000	30000

Table 8. Perforated plate parameters and viscous characteristic length design

	viscous characteristic length/Λ /um					
(a)δ =0.05 a = 2 mm t_p = 10 mm	20	50	100	150	200	250
(b)δ =0.15 a =1 mm t_p =5 mm	20	50	100	150	200	250

Porosity refers to the percentage of air in porous materials. High porosity is an important characteristic of porous materials, it gives porous materials a very large specific surface area which is conducive to thermal-viscous dissipation. Figure 6 shows the effect of porosity on the sound absorption

coefficient. With the increase of porosity, sound absorption peaks move to low frequency under both perforated plate conditions. For the L-perforated plate the maximum sound absorption coefficient almost always reaches 1 (Figure 6a), illustrating the excellent sound insulate properties. However, for the M-perforated plate, the maximum sound absorption coefficient decreases with the increase of porosity (Figure 6b).

The influence of porosity on the average sound absorption coefficient at low and medium frequencies are shown in Figure 6c and 6d. Obviously, for L-perforated plate, α_M increases and α_L decreases with the increase of porosity, while both α_L and α_M increase with increasing porosity for M-perforated plate. So for L-perforated plate, higher porosity has advantages in low frequency sound absorption and lower porosity has advantages in medium frequency sound absorption. For M-perforated plate, higher porosity has slight advantages in both low and medium frequency sound absorption.

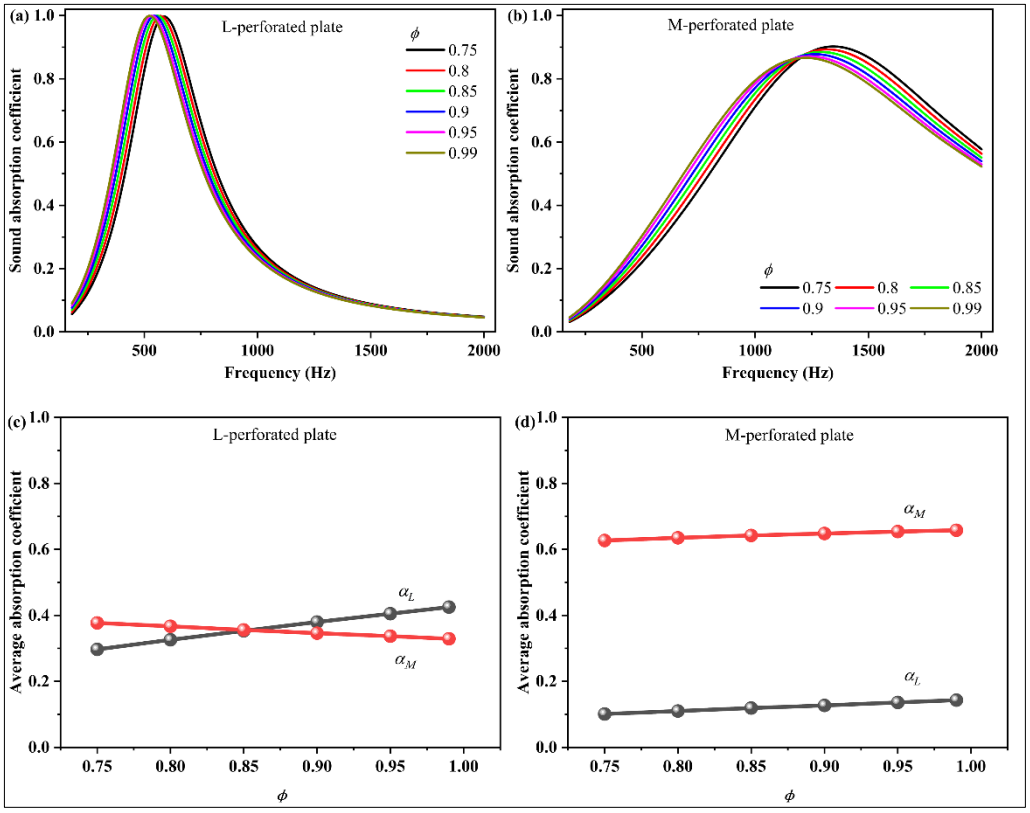

Figure 6. Influence of porosity on sound absorption coefficient for (a) L-perforated and (b) M-perforated plates, and the average absorption coefficient α_L and α_M as a function of ϕ for (c) L-perforated and (d) M-perforated plates

Tortuosity (or tortuosity factor) is used to describe the complexity of the propagation path of sound waves in porous materials, which is related to the microscopic geometric characteristics of porous materials [13]. It can be considered as the ratio of the actual average propagation path length of sound waves to the thickness of porous materials. Therefore, this value is usually greater than 1. Figure 7 shows the effect of tortuosity on sound absorption coefficient. Clearly, tortuosity has a relatively small effect on sound absorption coefficient of L-perforated plate with almost the same spectra profiles (Figure 7a). As for M-perforated plate shown in Figure 7b, sound absorption peak slightly moves to low frequency from 1230 to 1180 Hz and the maximum sound absorption coefficient also slightly increases from 0.87 to 0.88 with the increase of tortuosity. Similarly, the tortuosity has little influences on the average sound absorption coefficient of low and medium frequencies with unnoticeable variation of α_L and α_M values for both L-perforated and M-perforated plates (Figure 7c and 7d).

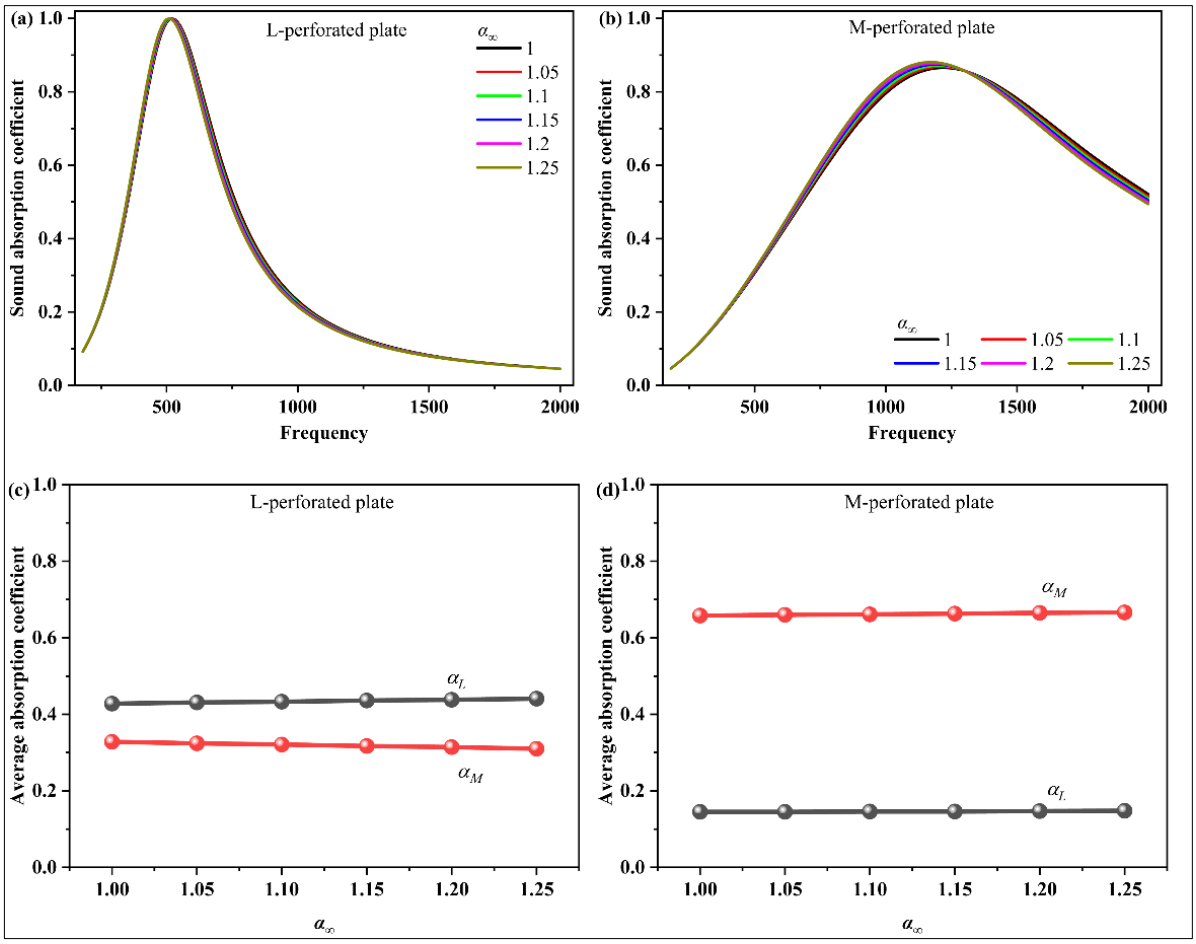

Figure 7. Influence of tortuosity on sound absorption coefficient for (a) L-perforated and (b) M-perforated plates, and the average absorption coefficient α_L and α_M as a function of α_∞ for (c) L-perforated and (d) M-perforated plates

Flow resistivity is a parameter that describes the resistance of a gas through a porous material, which is calculated by dividing the pressure difference per unit thickness by the linear velocity of the flow. The simulation results are shown in Figure 8. With the increase of flow resistivity, the maximum sound absorption coefficient of L-perforated plate decreases (Figure 8a). It is worth noting that the sound absorption coefficient increases when the frequency band below 400 Hz or above 800 Hz, implying enhanced sound adsorption performance of the composites in the low and middle frequency. The situation is totally different for M-perforated plate. As shown in Figure 8b, as the flow resistivity increases, the sound absorption coefficient of the whole frequency band is improved and the maximum sound absorption coefficient is significantly improved. When the flow resistivity is 20000 Pa·s/m², complete sound absorption can be achieved at 1200-1400 Hz. With the increase of flow resistivity, the complete sound absorption has a wider frequency band. Figure 8c and 8d show the influence of flow resistance on the average sound absorption coefficient of low and medium frequencies. With the increase of flow resistance, the α_L and α_M of L-perforated plate and M-perforated plate increase, but the α_L of L-perforated plate changes slightly when the flow resistance is between 20000 and 30000 Pa·s/m². That is to say, higher flow resistance is beneficial to the improvement of sound absorption performance of the two types of perforated plate.

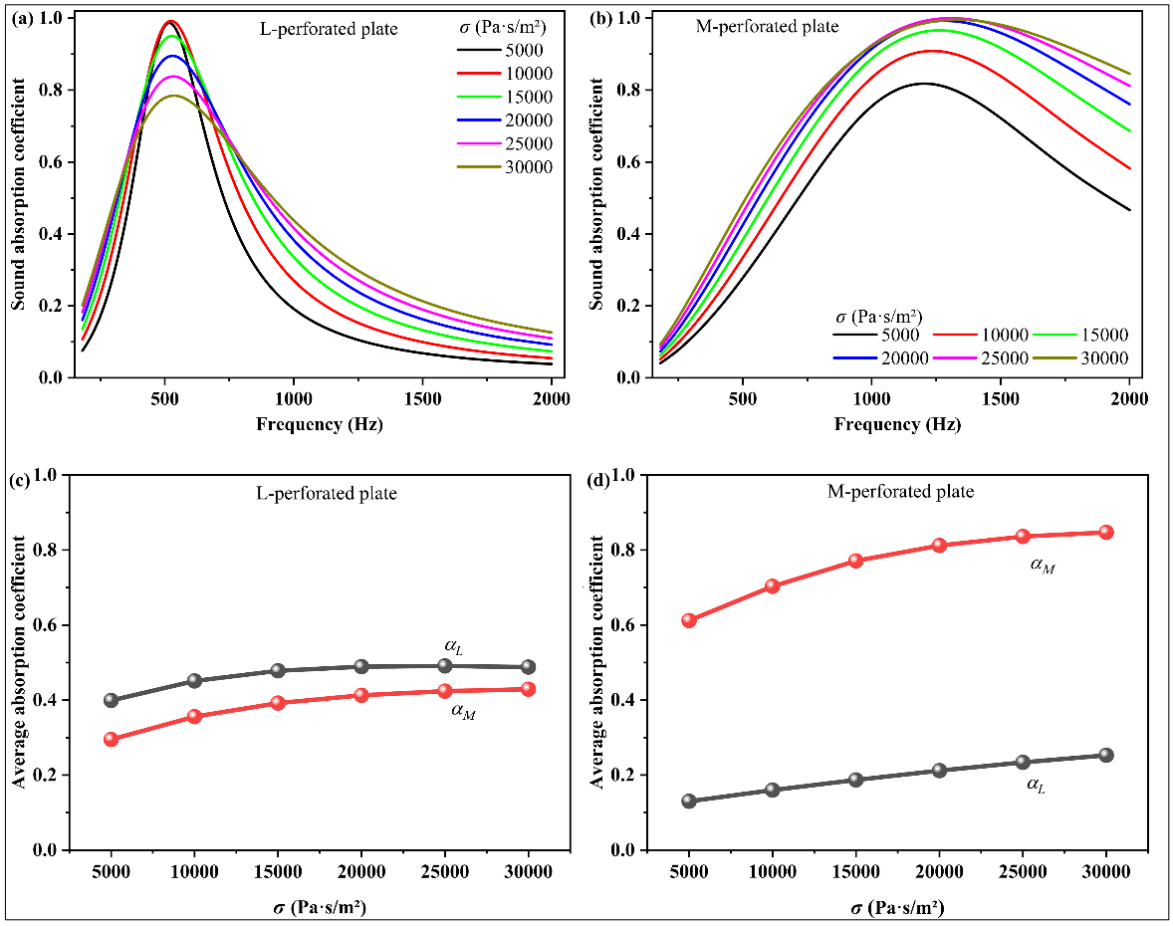

Figure 8. Influence of flow resistivity on sound absorption coefficient for (a) L-perforated and (b) M-perforated plates, and the average absorption coefficient αL and αM as a function of σ for (c) L-perforated and (d) M-perforated plates

The viscous characteristic length (Λ) is a parameter describing the viscous effect of acoustic wave propagation in porous materials [28,29]. When fluid flows in porous materials, the viscous effect causes the velocity gradient between fluids and the friction between fluids and porous material walls, resulting in viscous loss. For porous materials, viscous characteristic length is mainly related to the geometric characteristics of the holes, which can be understood as the average size of the channels connecting the holes. The results of simulation experiments are shown in Figure 9. As for L-perforated plates, the Λ in the range of 100-250 μm has almost no effect on the absorption coefficient curve (Figure 9a). When Λ = 20 μm, the resonance peak significantly moves towards the low frequency and the corresponding maximum absorption coefficient decreases. Figure 9b shows that the Λ in the range of 150~ 250 μm has little effect on the sound absorption coefficient curve for M-perforated plates. When the Λ continues to decrease, the resonance peak moves to the low frequency, and the maximum sound absorption coefficient is significantly improved. When Λ = 20 μm, the sound absorption coefficient is 0.99, illustrating that complete sound absorption can be achieved. Figure 9cd shows that there is no significant effect on the results when Λ is greater than 150 μm. For L-perforated plate as the Λ decrease α_L increase and α_M reduce, and for M-perforated plate as the Λ decrease both α_L and α_M are improved. We can conclude that when the length of viscous characteristic length is too high, it does not have much effect on the results. For L-perforated plate, the smaller length is favorable for low frequency sound absorption, and the larger length is favorable for medium frequency sound absorption. For M-perforated plate, the smaller length is favorable for low and medium frequency sound absorption.

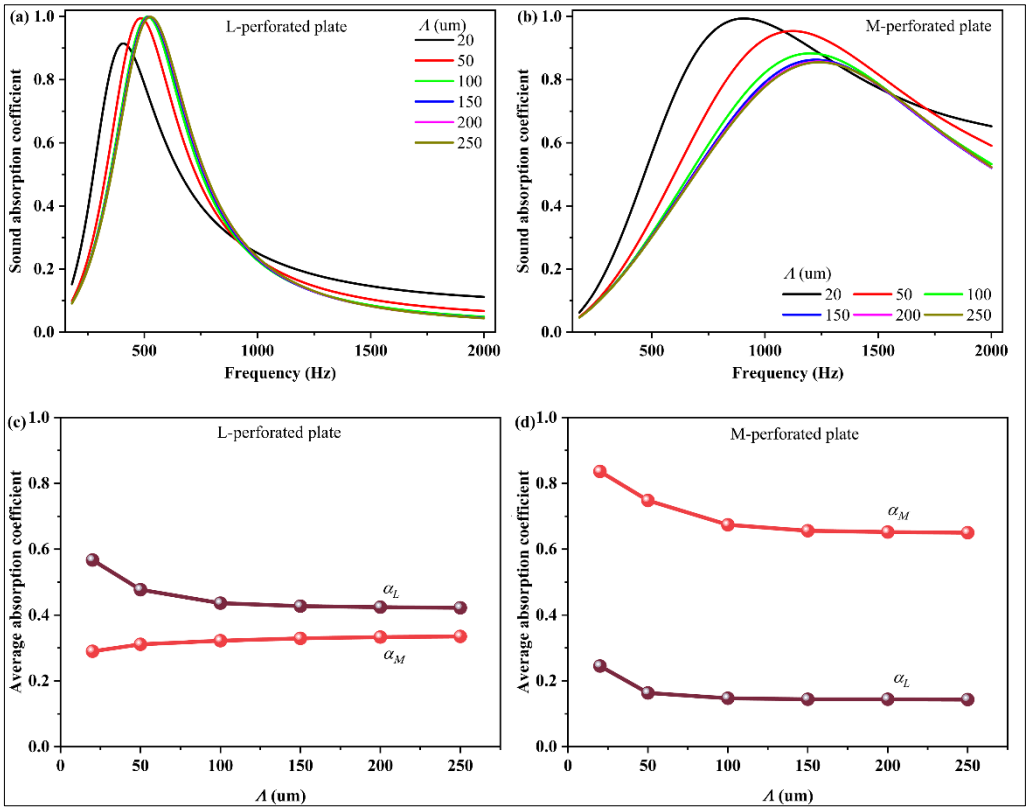

Figure 9. Influence of viscous characteristic length on sound absorption coefficient for (a) L-perforated and (b) M-perforated plates, and the average absorption coefficient α_L and α_M as a function of Λ for (c) L-perforated and (d) M-perforated plates

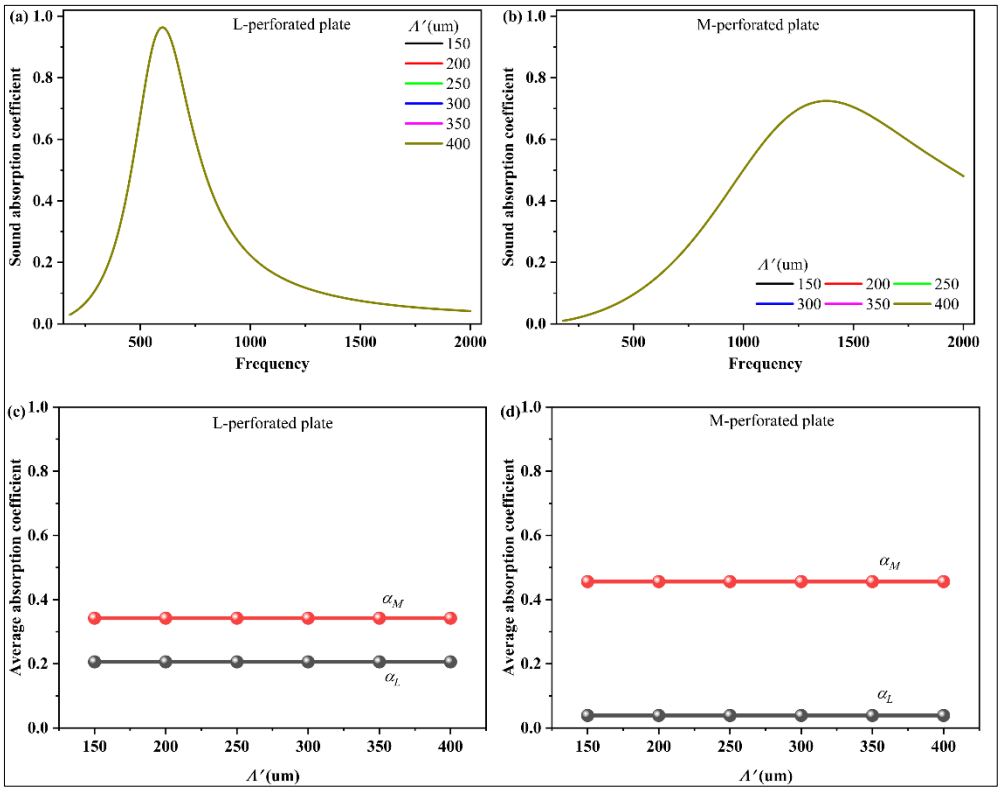

Figure 10. Influence of thermal characteristic length on sound absorption coefficient for (a) L-perforated and (b) M-perforated plates, and the average absorption coefficient α_L and α_M as a function of Λ' for (a) L-perforated and (b) M-perforated plates

3.2. Experimental verification

The practical composites composed of the perforated plate and the melamine foam was used to verify the numerical simulation results. Two kinds of perforated plates (named PP1 and PP2, respectively) were prepared by 3D printing (additive manufacturing). The 3D printing device is the Ultimaker, and the 3D printing material is PLA. The print core is AA 0.4, and the packing density is 100%. The parameters of the two kinds of perforated plates are shown in Table 10. The basic parameters for two melamine foams (LDMF and HDMF) are shown in Table 1. The numerical simulation results and the measured results are shown in Figure 11, with four groups for two perforated plates (PP1 and PP2) and two melamine foam (LDMF and HDMF).

Table 9. Perforated plate parameters and thermal characteristic length design

	thermal characteristic length/Λ'/um					
(a)δ =0.05 a = 2 mm t_p = 10 mm	150	200	250	300	350	400
(b)δ =0.15 a =1 mm t_p =5 mm	150	200	250	300	350	400

Table 10. Parameters of perforated plates

	a/mm	δ	t_p/mm
PP1	2.25	0.08	5.2
PP2	1.10	0.08	5.2

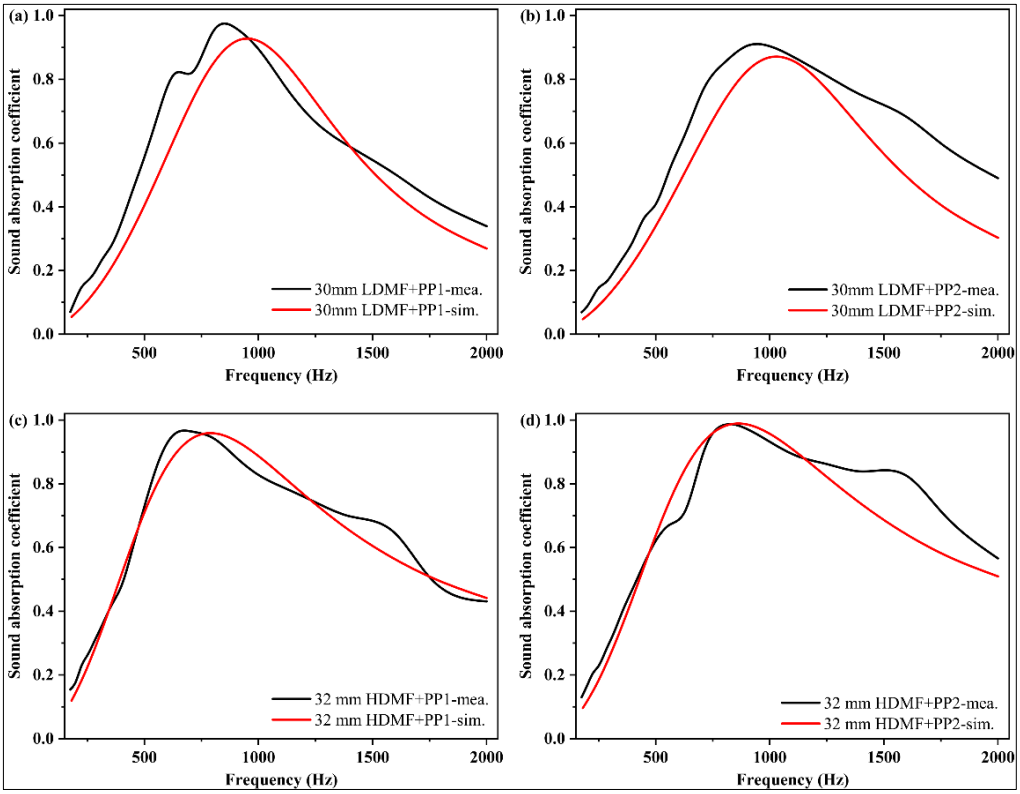

Figure 11. Measured (mea.) and simulated (sim.) sound absorption coefficients curves :(a) 30 mm LDMF+ PP1, (b) 30 mm LDMF+ PP2, (c) 32 mm HDMF+ PP1 and (d) 32 mm HDMF+ PP1

Figure 11 exhibits that the simulation results are roughly consistent with the measured results under the four combinations. The two combinations that contain PP2 show more errors when the frequencies are higher than 1000 Hz in Figure 11b and 1250 Hz in Figure 11d. The errors may be caused by the manufacturing of the perforated plate. In practical, the rough wall of the holes creates a part of heat dissipation through friction and viscosity, which makes the measured sound absorption coefficient

higher than the simulation results in some frequency bands. It must be emphasized that melamine foam is not a homogeneous material which caused some errors. Compared with the experimental and simulation data errors in other related studies [23, 30], the errors in this paper are acceptable. The validation experiment proves that it is reliable to use numerical simulation method to explore the influence of characteristic parameters of porous material and structural parameters of perforated plate on sound absorption performance. Accordingly, the simulation results can provide some guidelines for the design of the required composite structure in practical applications.

4. Conclusions

In this study, we established the finite element model of composite structure with perforated plate backed by porous materials and the JCA model is used to describe the acoustic characteristics. The influences of the characteristic parameters of melaine foam and the structural parameters of perforated plate on the sound absorption performance of the composite structure are investigated by numerical simulation. The results show that when we discuss perforated plates, lower perforation rate, larger aperture and thicker perforated plate are favorable for low frequency sound absorption, while higher perforation rate, smaller aperture and thinner perforated plate are favorable for medium frequency sound absorption. The effects of basic acoustic parameters on the sound absorption performance of the L-perforated plate and M-perforated plate are discussed separately. The tortuosity and thermal characteristic length have little influence on the results. For L-perforated plate and M-perforated plate, higher porosity, higher flow resistivity and smaller viscous characteristic length have advantages in low frequency sound absorption. For L-perforated plate, lower porosity, higher flow resistivity, larger viscous characteristic length have advantages in medium frequency sound absorption. For M-perforated plate, higher porosity, higher flow resistivity, smaller viscous characteristic length have advantages in medium frequency sound absorption.

Two kinds of perforated plates were prepared by 3D printing, respectively in the combination of LDHM and HDMF to form four groups of the composites. The comparison between the numerical simulation and the measured absorption coefficient curves proves that the numerical simulation method has good adaptability and high reliability. The obtained results are helpful to promote the development of porous material-perforated plate composite structure, and the appropriate parameter combination can be selected according to the frequency band of environmental noise.

Acknowledgements: This work was supported by Graduate Education Innovation Fund of Wuhan Institute of Technology (CX2020130) and National Natural Science Foundation of China (51273154).

References

1.NITU SA., SPOREA N., IATAN R., DURBACA I., VASILE O., CIOCOIU GC., Research on Obtaining Biocomposite Structures with Sound Absorbing Properties, *Mater. Plast.*, **59**(1), 2022, 131–7. https://doi.org/10.37358/mp.22.1.5566
2.DURBACA I., SPOREA N., VASILE O., Assessment of the Acoustic Absorption Characteristics of Layered Composite Structures Obtained from Plates with Lignocellulosic Coatings (I), *Mater. Plast.*, **57**(2), 2020, 8–14. https://doi.org/10.37358/MP.20.2.5345
3. CONSTANTIN M., CONSTANTIN L., ARADOAEI S., ARADOAEI M., BRATU M., VASILE O., Acoustic Properties of a New Composite Material Obtained from Feather Flour and Recycled Polypropylene, *Mater. Plast.*, **58**(4), 2021, 84–93. https://doi.org/10.37358/MP.21.4.5534
4.PERROT C., CHEVILLOTTE F., PANNETON R., Bottom-up approach for microstructure optimization of sound absorbing materials, *J Acoust Soc Am*, **124**(2), 2008, 940–8. https://doi.org/10.1121/1.2945115
5. MENG H., AO Q., REN SW., XIN F., TANG H., LU T., Anisotropic acoustical properties of sintered fibrous metals. *Compos Sci Technol*, **107**, 2015, 10–7. https://doi.org/10.1016/j.compscitech.2014.11.020

6. MENG H., YANG X., REN S., XIN F., LU T., Sound propagation in composite micro-tubes with surface-mounted fibrous roughness elements, *Compos Sci Technol*, **127**, 2016, 158–68. https://doi.org/10.1016/j.compscitech.2016.02.035
7. REN S., XIN F., LU TJ., ZHANG C., A semi-analytical model for the influence of temperature on sound propagation in sintered metal fiber materials, *Mater Des*, **134**, 2017, 513–22. https://doi.org/10.1016/j.matdes.2017.09.007
8. SAGARTZAZU X., HERVELLA L., PAGALDAY J., Review in Sound Absorbing Materials, *Arch Comput Methods Eng*, **15**(3), 2008, 311–42. https://doi.org/10.1007/s11831-008-9022-1
9. PARK J., MINN S., LEE H., YANG S., YU C., PAK S., OH C., SONG Y., KANG Y., YOUN J., Cell openness manipulation of low density polyurethane foam for efficient sound absorption, *J Sound Vib*, **406**, 2017, 224–36. https://doi.org/10.1016/j.jsv.2017.06.021
10. KIM B., CHO S., MIN D., PARK J., Experimental study for improving sound absorption of a composite helical-shaped porous structure using carbon fiber, *Compos Struct*, **145**, 2016, 242–7. https://doi.org/https://doi.org/10.1016/j.compstruct.2016.01.081
11. ALLARD J., CHAMPOUX Y., New empirical equations for sound propagation in rigid frame fibrous materials, *J Acoust Soc Am*, **91**(6), 1992, 3346–53. https://doi.org/10.1121/1.402824
12. JOHNSON D., KOPLIK J., DASHEN R., Theory of dynamic permeability and tortuosity in fluid saturated porous media, *J Fluid Mech*, **176**(1987), 1987, 379–402. https://doi.org/10.1017/S0022112087000727
13. CHAMPOUX Y., ALLARD J., Dynamic tortuosity and bulk modulus in air-saturated porous media, *J Appl Phys*, **70**(4), 1991, 1975–9. https://doi.org/10.1063/1.349482
14. GAO K., VAN DOMMELEN J., GEERS M., Microstructure characterization and homogenization of acoustic polyurethane foams: Measurements and simulations, *Int J Solids Struct*, **100**–**101**, 2016, 536–46. https://doi.org/10.1016/j.ijsolstr.2016.09.024
15.GAO K., VAN D., GEERS M., Investigation of the effects of the microstructure on the sound absorption performance of polymer foams using a computational homogenization approach, *Eur J Mech - A/Solids*, **61**, 2017, 330–44. https://doi.org/10.1016/j.euromechsol.2016.10.011
16. YANG X., REN S., WANG W., LIU X., XIN FX., LU T., A simplistic unit cell model for sound absorption of cellular foams with fully/semi-open cells, *Compos Sci Technol*, **118**(June), 2015, 276–83. https://doi.org/10.1016/j.compscitech.2015.09.009
17.NING J., ZHAO G., HE X., Non-acoustical parameters and sound absorption characteristics of porous polyurethane foams, *Phys Fluids*, **31**(3), 2019, 037106. https://doi.org/10.1063/1.5079486
18. ZHAI W., YU X., SONG X., ANG LYL., CUI F., LEE H., Microstructure-based experimental and numerical investigations on the sound absorption property of open-cell metallic foams manufactured by a template replication technique. *Mater Des*, **137**, 2018, 108–16. https://doi.org/10.1016/j.matdes.2017.10.016
19. OPIELA K., ZIELIŃSKI T., Microstructural design, manufacturing and dual-scale modelling of an adaptable porous composite sound absorber, *Compos Part B Eng*, **187**(February), 2020, 107833. https://doi.org/10.1016/j.compositesb.2020.107833
20.DESHMUKH S., RONGE H., RAMAMOORTHY S., Design of periodic foam structures for acoustic applications: Concept, parametric study and experimental validation, *Mater Des*, **175**, 2019, 107830. https://doi.org/10.1016/j.matdes.2019.107830
21.PARK J., YANG S., MINN K., YU C., PAK S., SONG Y., Design and numerical analysis of syntactic hybrid foam for superior sound absorption. *Mater Des*, **142**, 2018, 212–20. https://doi.org/10.1016/j.matdes.2018.01.040
22.TAYONG R., On the holes interaction and heterogeneity distribution effects on the acoustic properties of air-cavity backed perforated plates, *Appl Acoust*, **74**(12), 2013, 1492–8. https://doi.org/10.1016/j.apacoust.2013.05.016

23. WANG J., RUBINI P., QIN Q., Application of a porous media model for the acoustic damping of perforated plate absorbers, *Appl Acoust*, **127**, 2017, 324–35.
https://doi.org/10.1016/j.apacoust.2017.07.003
24. JIANG C., LI X., CHENG W., LUO Y., XING T., Acoustic impedance of microperforated plates with stepwise apertures, *Appl Acoust*, **157**, 2020, 106998.
https://doi.org/10.1016/j.apacoust.2019.106998
25.LI L., GANG X., LIU Y., ZHANG X., ZHANG F., Numerical simulations and experiments on thermal viscous power dissipation of perforated plates, *AIP Adv*, **8**(10), 2018, 105221.
https://doi.org/10.1063/1.5044705
26. CARBAJO J., RAMIS J., GODINHO L., AMADO P., Perforated panel absorbers with micro-perforated partitions. *Appl Acoust*, **149**, 2019, 108–13. https://doi.org/10.1016/j.apacoust.2019.01.023
27. GAI X., XING T., LI X., ZHANG B., WANG F., CAI Z., Sound absorption of microperforated panel with L shape division cavity structure, *Appl Acoust*, **122**, 2017, 41–50.
https://doi.org/10.1016/j.apacoust.2017.02.004
28.KIM KH., YOON GH, Absorption performance optimization of perforated plate using multiple-sized holes and a porous separating partition, *Appl. Acoust*, **120**, 2017, 21–33.
http://dx.doi.org/10.1016/j.apacoust.2017.01.004
29.MIN H., GUO W., Sound absorbers with a micro-perforated panel backed by an array of parallel-arranged sub-cavities at different depths, *Appl. Acoust*, 149, 2019, 123–128.
https://doi.org/10.1016/j.apacoust.2019.01.013
30.LI D., CHANG D., LIU B., Enhanced low- to mid-frequency sound absorption using parallel-arranged perforated plates with extended tubes and porous material, *Appl Acoust*, **127**, 2017, 316–23.
https://doi.org/10.1016/j.apacoust.2017.06.019
31.COX T., D'ANTONIO P., Acoustic Absorbers and Diffusers, *CRC Press*, 2016.
https://doi.org/10.1201/9781315369211

Manuscript received: 31.05.2022